Effect of the symmetry energy on nuclear stopping and its relation to the production of light charged fragments

Sanjeev Kumar and Suneel Kumar*
School of Physics and Material Science, Thapar University, Patiala 147004, Punjab, India

Rajeev K. Puri
Department of Physics, Panjab University, Chandigarh-160014, India
(Received 3 June 2009; published 6 January 2010)

We present a complete systematics (excitation function, impact parameter, system size, isospin asymmetry, and equations of state dependences) of global stopping and fragment production for heavy-ion reactions in the energy range between 50 and 1000 MeV/nucleon in the presence of symmetry energy and an isospin-dependent cross section. It is observed that the degree of stopping depends weakly on the symmetry energy and strongly on the isospin-dependent cross section. However, the symmetry energy and isospin-dependent cross section has an effect of the order of more than 10% on the emission of light charged particles (LCP's). It means that nuclear stopping and LCP's can be used as a tool to get the information of an isospin-dependent cross section. Interestingly, the LCP's emission in the presence of symmetry energy is found to be highly correlated with the global stopping.

DOI: 10.1103/PhysRevC.81.014601 PACS number(s): 25.70.Pq, 21.65.Ef

I. INTRODUCTION

One of the goals of heavy-ion collisions (HIC) at intermediate energies is to extend the knowledge of hot and dense nuclear matter to the extreme conditions. In the past, these studies were focused on multifragmentation that constituted fragments of all sizes [1]. An additional promising observable for the understanding of nuclear equation of state is the anisotropy in the momentum distribution that includes the directed in-plane flow (bounce off) as well as out-of-plane flow (squeeze out) [2,3]. The absolute values of the flow results from the interplay between the attractive mean field and repulsive nucleon-nucleon scatterings. This interplay is also responsible for the transition from a fused state to one of total disassembly. Another phenomena linked with the above interplay is the global stopping of nuclear matter. Recently, Puri *et al.* [4] tried to correlate the multifragmentation with global nuclear stopping. Their findings revealed that light charged particles act in a similar fashion as the anisotropy ratio. They, however, did not take isospin of the system into account.

Following the recent development of radioactive beam facilities in many parts of the world, it became possible to study the neutron (or proton) rich nuclear collisions at intermediate energies. Therefore, for a meaningful investigation, one should include the isospin dependence of the field. As pointed out by Bauer [5], nuclear stopping at intermediate energies is determined by the mean field as well as by the in-medium NN cross sections. Unfortunately, his calculations were silent about the symmetry potential. The recent work of many authors [6–8] suggested that the degree of approaching isospin equilibration helps to probe the nuclear stopping in HIC. In Ref. [7], the isospin dependence of a cross section was investigated in nuclear stopping. In a recent communication [8], authors studied the behavior of the excitation function Q_{zz}/nucleon and concluded that Q_{zz}/nucleon can provide information about the isospin dependence in terms of cross sections. Several more studies also focused in recent years on the isospin degree of freedom [9].

We wish to focus on the systematic study of isospin dependence and will focus on the relation between light charged particles and equilibration of the reaction using isospin-dependent quantum molecular dynamics.

This study is done within the framework of an isospin-dependent quantum molecular dynamics model that is explained in Sec. II. The results are presented in Sec. III. We present the summary in Sec. IV.

II. ISOSPIN-DEPENDENT QUANTUM MOLECULAR DYNAMICS MODEL

The isospin-dependent quantum molecular dynamics (IQMD) [10] model treats different charge states of nucleons, deltas, and pions explicitly [11], as inherited from the Vlasov-Uehling-Uhlenbeck (VUU) model [12]. The IQMD model was used successfully for the analysis of a large number of observables from low to relativistic energies [10,11,13]. The isospin degree of freedom enters into the calculations via both cross sections and mean field [12,14]. The details about the elastic and inelastic cross sections for proton-proton and neutron-neutron collisions can be found in Refs. [10,13].

In this model, baryons are represented by Gaussian-shaped density distributions

$$f_i(\vec{r},\vec{p},t) = \frac{1}{\pi^2\hbar^2} e^{-[\vec{r}-\vec{r}_i(t)]^2\frac{1}{2L}} e^{-[\vec{p}-\vec{p}_i(t)]^2\frac{2L}{\hbar^2}}. \quad (1)$$

Nucleons are initialized in a sphere with radius $R = 1.12A^{1/3}$ fm, in accordance with the liquid drop model. Each nucleon occupies a volume of h^3 so that phase space is uniformly

*suneel.kumar@thapar.edu

filled. The initial momenta are randomly chosen between 0 and Fermi momentum (p_F). The nucleons of the target and projectile interact via two and three-body Skyrme forces and the Yukawa potential. The isospin degree of freedom is treated explicitly by employing a symmetry potential and explicit Coulomb forces between protons of the colliding target and projectile. This helps in achieving the correct distribution of protons and neutrons within the nucleus.

The hadrons propagate using Hamilton equations of motion

$$\frac{dr_i}{dt} = \frac{d\langle H\rangle}{dp_i}; \quad \frac{dp_i}{dt} = -\frac{d\langle H\rangle}{dr_i}, \tag{2}$$

with

$$\begin{aligned}\langle H\rangle &= \langle T\rangle + \langle V\rangle \\ &= \sum_i \frac{p_i^2}{2m_i} + \sum_i \sum_{j>i} \int f_i(\vec{r},\vec{p},t) V^{ij}(\vec{r}',\vec{r}) \\ &\quad \times f_j(\vec{r}',\vec{p}',t) d\vec{r} d\vec{r}' d\vec{p} d\vec{p}'. \end{aligned} \tag{3}$$

The baryon-baryon potential V^{ij}, in the earlier relation, reads as

$$\begin{aligned} V^{ij}(\vec{r}'-\vec{r}) &= V^{ij}_{\text{Skyrme}} + V^{ij}_{\text{Yukawa}} + V^{ij}_{\text{Coul}} + V^{ij}_{\text{sym}} \\ &= \left[t_1 \delta(\vec{r}'-\vec{r}) + t_2 \delta(\vec{r}'-\vec{r}) \rho^{\gamma-1} \left(\frac{\vec{r}'+\vec{r}}{2} \right) \right] \\ &\quad + t_3 \frac{\exp(|\vec{r}'-\vec{r}|/\mu)}{(|\vec{r}'-\vec{r}|/\mu)} + \frac{Z_i Z_j e^2}{|\vec{r}'-\vec{r}|} \\ &\quad + t_6 \frac{1}{\varrho_0} T_3^i T_3^j \delta(\vec{r}_i{}' - \vec{r}_j). \end{aligned} \tag{4}$$

Here Z_i and Z_j denote the charges of ith and jth baryons and T_3^i, and T_3^j are their respective T_3 components (i.e., $1/2$ for protons and $-1/2$ for neutrons). The Meson potential consists of a Coulomb interaction only. The parameters μ and $t_1, \ldots, t_6$ are adjusted to the real part of the nucleonic optical potential. For the density dependence of the nucleon optical potential standard Skyrme-type parametrization is employed. The choice of equation of state (or compressibility) is still a controversial one. Many studies advocated softer matter, whereas many more believed the matter to be harder in nature [12,15]. We shall use both hard (H) and soft (S) equations of state that have compressibilities of 380 and 200 MeV, respectively.

The binary nucleon-nucleon collisions are included by employing the collision term of the well-known VUU-Boltzmann-Uehling-Uhlenbeck (BUU) equation [2,12]. The binary collisions are done stochastically, in a similar way as are done in all transport models. During the propagation, two nucleons are supposed to suffer a binary collision if the distance between their centroids

$$|r_i - r_j| \leqslant \sqrt{\frac{\sigma_{\text{tot}}}{\pi}}, \quad \sigma_{\text{tot}} = \sigma(\sqrt{s}, \text{type}), \tag{5}$$

"type" denotes the ingoing collision partners (N-N, N-Δ, N-π, etc.). In addition, Pauli blocking (of the final state) of baryons is taken into account by checking the phase space densities in the final states. The final phase space fractions P_1 and P_2, which are already occupied by other nucleons, are determined for each of the scattering baryons. The collision is then blocked with probability

$$P_{\text{block}} = 1 - (1 - P_1)(1 - P_2). \tag{6}$$

The delta decays are checked in an analogous fashion with respect to the phase space of the resulting nucleons.

III. RESULTS AND DISCUSSION

The global stopping in HIC was studied with the help of many different variables. In earlier studies, one used to relate the rapidity distribution with global stopping. The rapidity distribution can be defined as [4,16]

$$Y(i) = \frac{1}{2} ln \frac{E(i) + p_z(i)}{E(i) - p_z(i)}, \tag{7}$$

where $E(i)$ and $p_z(i)$ are, respectively, the total energy and longitudinal momentum of the ith particle. For a complete stopping one expects a single Gaussian shape. Obviously, narrow Gaussian indicate better thermalization compared to broader Gaussian.

The second possibility to probe the degree of stopping is the anisotropy ratio (R) [7]

$$R = \frac{2}{\pi} \frac{[\sum_i |p_\perp(i)|]}{[\sum_i |p_\parallel(i)|]}, \tag{8}$$

where the summation runs over all nucleons. The transverse and longitudinal momenta are $p_\perp(i) = \sqrt{p_x^2(i) + p_y^2(i)}$ and $p_\parallel(i) = p_z(i)$, respectively. Naturally, for a complete stopping R should be close to unity.

Another quantity, which is an indicator of nuclear stopping and was used recently, is the quadrupole moment Q_{zz}, defined as [7]

$$Q_{zz} = \sum_i \left[2p_z^2(i) - p_x^2(i) - p_y^2(i) \right]. \tag{9}$$

Naturally, for a complete stopping, Q_{zz} should be close to zero.

In the present analysis, thousands of events were simulated for the neutron-rich reaction of ${}_{54}\text{Xe}^{131} + {}_{54}\text{Xe}^{131}$ at incident energies between 50 and 1000 MeV/nucleon using a hard equation of state along with energy dependent Cugnon and constant nucleon-nucleon cross sections [17]. Moreover, to see the effect of compressibilities on nuclear stopping and fragmentation soft equation of state is also used in Fig. 5. The geometry of the collision was varied between the most central to the peripheral one. The role of symmetry energy is studied by simulating the previous reaction with and without this term. As stated earlier, we plan to study the degree of stopping and emission of fragments using symmetry energy and an isospin-dependent cross section. We shall also correlate the degree of stopping with the emission of light charged particles as is also done in Ref. [4]. The fragments are constructed within the minimum spanning tree (MST) method [1], which binds nucleons if they are within a distance of 4 fm.

In Fig. 1, we display the final phase space of a single event of ${}_{54}\text{Xe}^{131} + {}_{54}\text{Xe}^{131}$ at an incident energy of 400 MeV/nucleon with and without symmetry energy. The top, middle, and bottom panels are at $\hat{b} = 0$, 0.3 and 0.6,

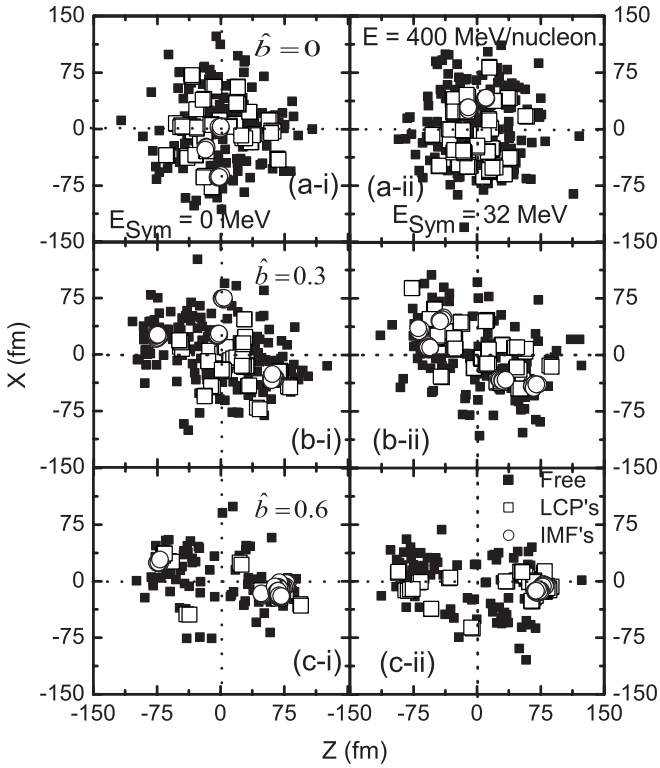

FIG. 1. The final phase space of a single event for the reaction of $_{54}Xe^{131} + _{54}Xe^{131}$ with (ii) and without symmetry energy (i). The top (a), middle (b), and bottom (c) panels are, respectively, for scaled impact parameters $\hat{b} = 0$, 0.3, and 0.6. Different symbols are for free nucleons, LCP's, and IMF's.

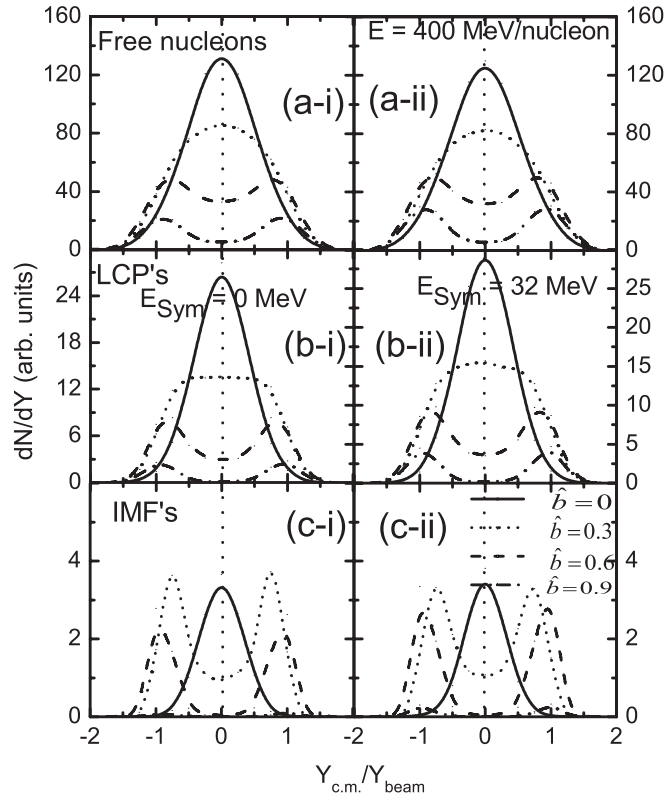

FIG. 2. The rapidity distribution dN/dY as a function of reduced rapidity for free nucleons (a), LCP's (b), and IMF's (c) at different impact parameters. The reaction under study is $_{54}Xe^{131} + _{54}Xe^{131}$ at incident energy $E = 400$ MeV/nucleon. The left and right panels are with (ii) and without symmetry energy (i).

respectively. Here the phase space of free particles [$A = 1$], light charged particles (LCP's) [$2 \leqslant A \leqslant 4$], and intermediate mass fragments (IMF's) [$5 \leqslant A \leqslant 44$] is displayed. We note that irrespective of the symmetry energy, the central collisions lead to a complete spherical distribution of particles, indicating the spreading of the nucleons in all directions. It means that the breaking of initial correlations among nucleons is maximal in this region and, as a result, more randomization and stopping in the hot and compressed nuclear matter occurs. This effect seems to decrease with the impact parameter. Since free particles as well as LCP's originate from the midrapidity region they are better suited for studying the degree of stopping reached in an HIC. However, IMF's seem to originate either from the target or from the projectile region, therefore, are the remnant/residue of the spectator matter. This observation is in agreement with many other studies [1,4,18].

To further quantify this observation, we display in Fig. 2, the rapidity distribution $\frac{dN}{dY}$ for the emission of free nucleons as well as LCP's and IMF's. We see that free particles and LCP's emitted in the central collisions form a single narrow Gaussian shape, whereas IMF's have broader Gaussian indicating less thermalization. As we increase the impact parameter, the single Gaussian distribution splits into two Gaussian (at target and projectile rapidities), indicating correlated matter. From the shape of the Gaussian, one sees that free particles and LCP's are a better indicator of the thermal source. Obviously, this condition is necessary, but not a sufficient one.

From the figure it is also evident that the symmetry energy does not play a significant role for the rapidity distribution. The peak value of the Gaussian for LCP's is altered by about 10%, whereas nearly no effect is seen in the case of IMF's. The reason is that LCP's can feel the role of mean field directly while the heavy fragments have weak sensitivity [19]. From the figure, one sees a one to one relation between the degree of stopping and the emission of LCP's. These conclusions match with the findings of Fig. 1 and Ref. [4].

In Fig. 3, we display the impact parameter dependence of global variables (R and Q_{zz}/nucleon), whereas the multiplicity dependence of free nucleons and LCP's is displayed in Fig. 4. The displayed results are at $E_{\rm Sym} = 0$ and $E_{\rm Sym} = 32$ MeV in each panel while in panel (b) the results are also displayed with an isospin-dependent cross section. The value of a cross section is denoted in the superscript. From Fig. 3 we observe that R and Q_{zz}/nucleon behave in opposite fashions (i.e., R and $\frac{1}{Q_{zz}/\text{nucleon}}$ will behave in a similar fashion). For $R > 1$ and $Q_{zz}/\text{nucleon} < 0$, it can be explained by the preponderance of momentum flow perpendicular to the beam direction [20]. The maximum stopping is observed around 400 MeV/nucleon, which is in supportive nature with the findings of Reisdorf *et al.* [21]. In their work, they measured the nuclear stopping from 0.090 to 1.93 GeV/nucleon and maximal stopping was observed around 400 MeV/nucleon. It is clear that if the reaction reaches the maximal stopping around certain energies,

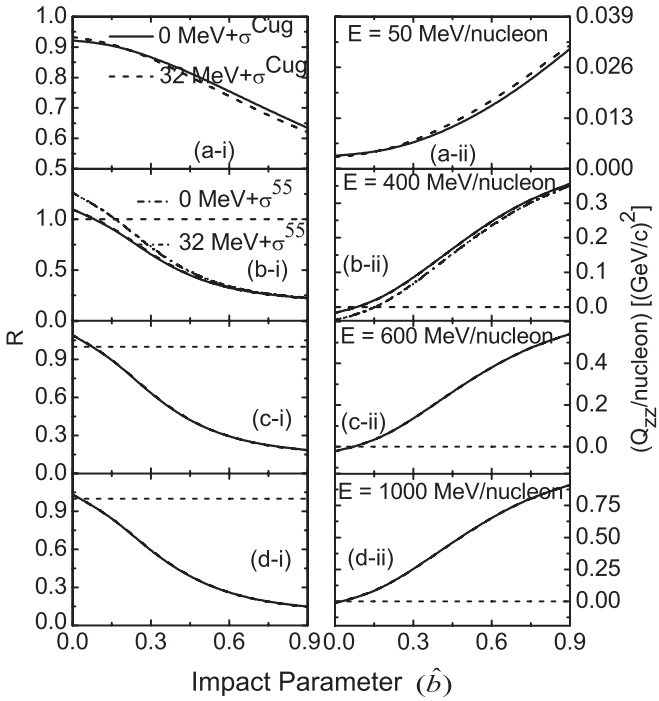

FIG. 3. The anisotropy ratio R (i) and quadrupole moment (Q_{zz}/nucleon) (ii) as a function of the normalized impact parameters with and without symmetry energy. In panel (b) the results are also displayed with isospin-dependent cross section (55 mb). The panels from top to bottom are at incident energies of (a) 50, (b) 400, (c) 600, and (d) 1000 MeV/nucleon, respectively.

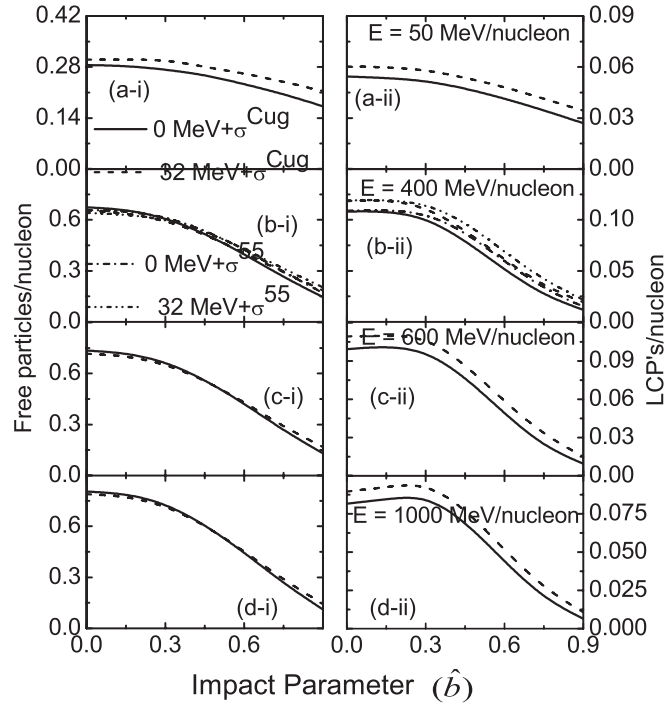

FIG. 4. Same as in Fig. 3, but for the multiplicity of free particles/nucleon and LCP's/nucleon.

the matter formed in the reaction should reach minimum transparency and thus most of the particles are preferentially out of plane. However, no visible effect is seen for the symmetry energy term. We see both quantities are nearly independent of the symmetry energy while strongly dependent on the isospin-dependent cross section.

As we know, the major contribution for the stopping of nuclear matter is from the hot and compressed regions where symmetry energy does not play any role. Some small spikes can be seen at lower beam energies, however, the outcome is independent of the symmetry energy at higher incident energies. This is due to the fact that above the Fermi energy, incident energy itself is sufficient to break the initial correlations among the nucleons. However, the isospin-dependent cross section will lead to violent N-N collisions, which further cause the transformation of the initial longitudinal motion in other directions and hence thermalization of the system. This dominant role played by the isospin-dependent cross section gradually disappears with the increase in the impact parameter. As discussed earlier, stopping is the phenomenon that originates from the participant zone and this zone goes on decreasing with the increase in the impact parameter and hence the effect of the cross section on nuclear stopping. These findings are also in supportive nature with the findings of Liu *et al.* [7].

To correlate the degree of stopping with the multiplicity of fragments, we display in Fig. 4 the impact parameter dependence of the multiplicity of free nucleons as well as of LCP's. The behavior of all curves is similar to that of nuclear stopping parameters R and $\frac{1}{Q_{zz}/\text{nucleon}}$, as discussed in Fig. 3. In addition, LCP's are more sensitive toward symmetry energy compared to free particles. Due to the pairing nature of LCP's, the symmetry energy term $\propto (N-Z)^2$ contributes considerably. The effect of the isospin-dependent cross section is more visible for the LCP's as compared to free particles. This also gives us a clue that the LCP's production can act as an indicator for the nuclear stopping. Moreover, free particles/nucleon are found to increase monotonically with the incident energy while LCP's/nucleon behave in a similar fashion as that of nuclear stopping (i.e., maximum around 400 MeV/nucleon and then decreases). It is also evident from Ref. [4], the production of LCP's act as a barometer for nuclear stopping compared to the free particles.

In Fig. 5, we checked the sensitivity of nuclear stopping as well as fragment production with the nuclear equation of state (EOS). For this purpose, a hard (H) and soft (S) EOS with compressibility $\kappa = 380$ and 200 MeV are employed, respectively. The nuclear stopping is found to be weakly dependent on the EOS while the fragment production is sensitive to different EOS. It means that the fragment production with different EOS can act as a global indicator for the nuclear stopping as it is weakly dependent on EOS.

It also becomes important to study the system size dependence and isospin asymmetry of R, $\frac{1}{Q_{zz}/\text{nucleon}}$, free particles, and LCP's. For this, in Fig. 6, we display the results for the reactions of $_{20}Ca^{40} + _{20}Ca^{40}$, $_{28}Ni^{58} + _{28}Ni^{58}$, $_{41}Nb^{93} + _{41}Nb^{93}$, $_{54}Xe^{131} + _{54}Xe^{131}$, and $_{79}Au^{197} + _{79}Au^{197}$, in which Z as well as A are varied. However, results are displayed in Fig. 7 for the reactions of $_{20}Ca^{34} + _{20}Ca^{34}$ ($N/Z = 0.7$), $_{20}Ca^{40} + _{20}Ca^{40}$ ($N/Z = 1$), $_{20}Ca^{48} + _{20}Ca^{48}$

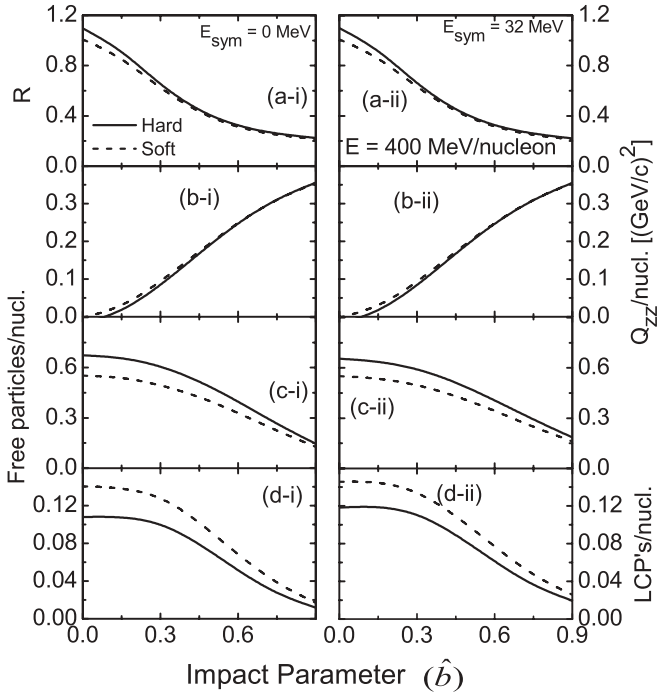

FIG. 5. Impact parameter dependence of (a) R, (b) Q_{zz}/nucleon, (c) free particles/nucleon, and (d) LCP's/nucleon with hard (H) and soft (S) equations of state. The results are displayed at $E_{\rm Sym} = 0$ (i) and 32 MeV (ii).

$(N/Z = 1.4)$, and $_{20}Ca^{57} + {}_{20}Ca^{57}$ $(N/Z = 1.85)$ having the same Z and different A in the presence of symmetry energy and the isospin-dependent cross section. The curves in Figs. 6 and 7 are parametrized with the power law $Y = CX^{\tau}$, where C and

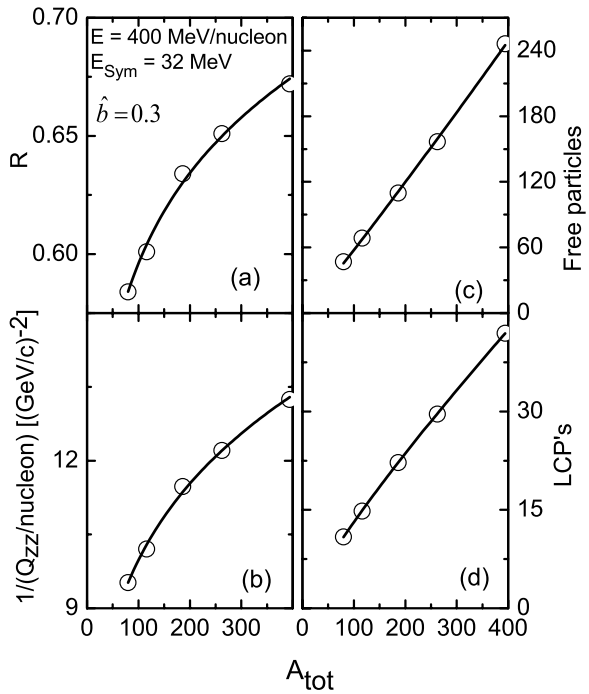

FIG. 6. System size dependence of (a) R, (b) $\frac{1}{Q_{zz}/\text{nucleon}}$, (c) free particles, and (d) LCP's in the presence of symmetry energy. All the curves are fitted with a power law.

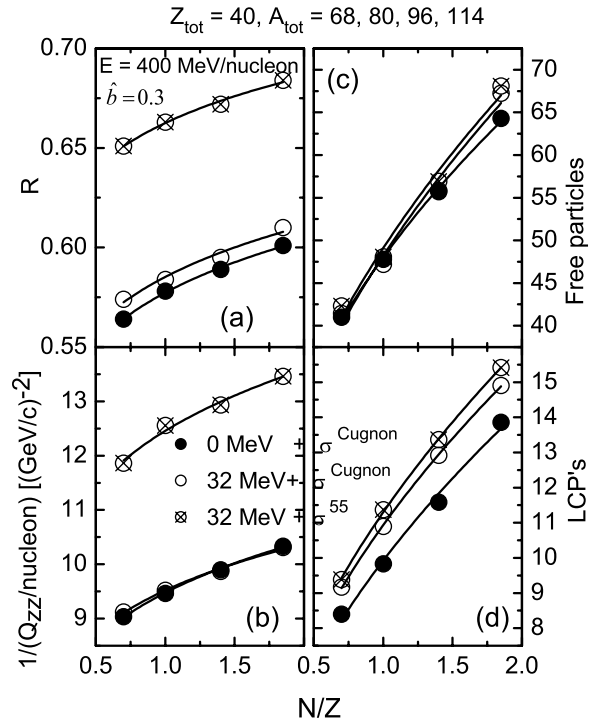

FIG. 7. Isospin asymmetry of (a) R, (b) $\frac{1}{Q_{zz}/\text{nucleon}}$, (c) free particles, and (d) LCP's in the presence of symmetry energy and the isospin-dependent cross section (55 mb).

τ are constants while X and Y are the respective parameters on the X and Y axes.

From Fig. 6 it is observed that the parameters R, $\frac{1}{Q_{zz}/\text{nucleon}}$, free particles, as well as LCP's are in similar trend with the composite mass of the system. All the parameters are found to increase with the composite mass of the system. For a fixed geometry (semicentral here), the composite system is heavier and the compressed zone is hotter, which further results in more thermalization or global stopping. Looking at the parallel side, the free particles and LCP's will always originate from the participant zone. With an increase in the composite mass of the system, the participant zone goes on increasing for a fixed geometry (semicentral here) and hence the production of free particles and LCP's. Similar findings are also published in Refs. [7,22].

The dependence of these parameters on the isospin asymmetry (N/Z dependence) displayed in Fig. 7 is also found to be in supportive nature with the findings in Fig. 6. An increase in the number of neutrons will increase the number of collisions and hence the dominance of R, $\frac{1}{Q_{zz}/\text{nucleon}}$, free particles, as well as LCP's is observed with the increase in the N/Z ratio. Nuclear stopping as well as LCP's are observed to be strongly dependent on the isospin-dependent cross section. Similar results with the isospin-dependent cross section are observed in Figs. 3 and 4. From here one may conclude that the nuclear stopping and LCP's can also be used as a tool to investigate the isospin-dependent cross section.

To further elaborate this point, we display in Fig. 8 multiplicity/nucleon (free and LCP's) as well as R and $\frac{1}{Q_{zz}/\text{nucleon}}$. Once free nucleons and LCP's are normalized with

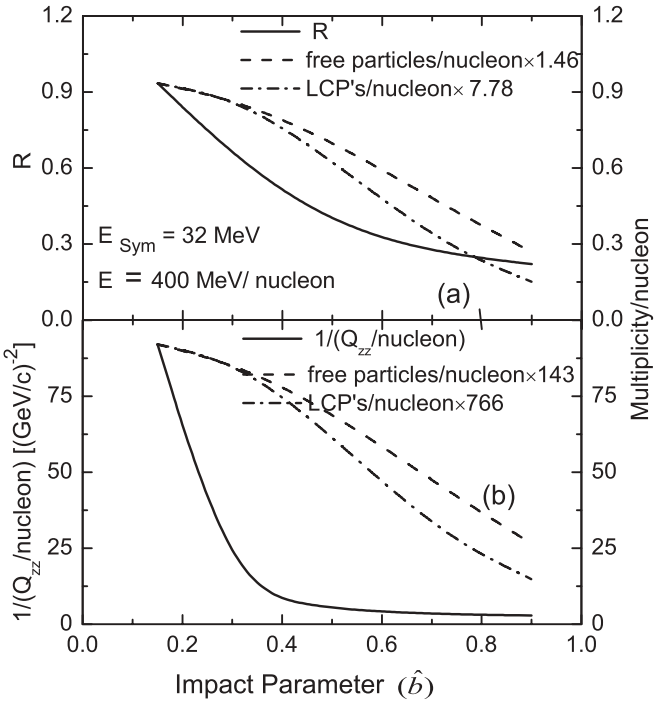

FIG. 8. The scaled free particles/nucleon and LCP's/nucleon along with anisotropy ratio R (a) and $\frac{1}{Q_{zz}/\text{nucleon}}$(b) as a function of normalized impact parameter in the presence of symmetry energy. The reaction is at incident energy 400 MeV/nucleon.

R at the starting point of the impact parameter, we see that their behavior with respect to the impact parameter is similar to that of the anisotropy ratio, whereas a visible difference occurs with reference to the quadrupole moment. This similarity in all three quantities in the presence of symmetry energy makes LCP's a good indicator of global stopping in HIC.

IV. CONCLUSION

In summary, using the IQMD model, we investigate the emission of free particles, LCP's, and the degree of stopping reached in HIC in the presence of symmetry energy and the isospin-dependent cross section. We observe that nuclear stopping in terms of the anisotropy ratio and quadrupole moment depends weakly on the symmetry energy and strongly on the isospin-dependent cross section. However, the symmetry energy and isospin-dependent cross section have an effect of 10% on the production of LCP's. This means that nuclear stopping and LCP's production can be used as a tool to investigate the isospin-dependent cross section. The LCP's production is found to be highly correlated with global stopping.

ACKNOWLEDGMENTS

This work was supported by Grant No. 03(1062)06/ EMR-II from the Council of Scientific and Industrial Research (CSIR), New Delhi, Govt. of India.

[1] J. Singh, S. Kumar, and R. K. Puri, Phys. Rev. C **62**, 044617 (2000); **63**, 054603 (2001); A. Le Fevre and J. Aichelin, Phys. Rev. Lett. **100**, 042701 (2008); Y. K. Vermani and R. K. Puri, Eur. Phys. Lett. **85**, 62001 (2009); S. Kumar, S. Kumar, and R. K. Puri, Phys. Rev. C **78**, 064602 (2008).

[2] H. Stöcker and W. Greiner, Phys. Rep. **137**, 277 (1986); A. D. Sood and R. K. Puri, Phys. Rev. C **69**, 054612 (2004); D. J. Magestro, W. Bauer, O. Bjarki, J. D. Crispin, M. L. Miller, M. B. Tonjes, A. M. VanderMolen, G. D. Westfall, R. Pak, and E. Norbeck, Phys. Rev. C **61**, 021602(R) (2000); P. Danielewicz, R. Lacey, and W. G. Lynch, Science **298**, 1592 (2002); J. Lukasik *et al.*, Phys. Lett. **B608**, 223 (2005); X. F. Luo, M. Shao, X. Dong, and C. Li, Phys. Rev. C **78**, 031901 (2008).

[3] J. Aichelin, Phys. Rep. **202**, 233 (1991).

[4] J. K. Dhawan, N. Dhiman, A. D. Sood, and R. K. Puri, Phys. Rev. C **74**, 057901 (2006), and the references within; P. B. Gossiaux and J. Aichelin, Phys. Rev. C **56**, 2109 (1997).

[5] W. Bauer, Phys. Rev. Lett. **61**, 2534 (1988); G. F. Bertsch, G. E. Brown, V. Koch, and B. A. Li, Nucl. Phys. **A490**, 745 (1998).

[6] B. A. Li and S. J. Yennello, Phys. Rev. C **52**, R1746 (1995); H. Johnston, T. White, J. Winger, D. Rowland, B. Hurst, F. Gimeno-Nogues, D. Okelly, and S. J. Yennello, Phys. Lett. **B371**, 186 (1996); B. A. Li, C. M. Ko, and W. Bauer, Int. J. Mod. Phys. E **7**, 147 (1998); S. J. Yennello *et al.*, Phys. Lett. **B321**, 15 (1994).

[7] J. Y. Liu, W. J. Guo, S. J. Wang, W. Zuo, Q. Zhao, and Y. F. Yang, Phys. Rev. Lett. **86**, 975 (2001).

[8] L. Q. Feng and L. Z. Xia, Chin. Phys. Lett. **19**, 321 (2002).

[9] J. Y. Liu, W. J. Guo, Y. Z. Xing, X. G. Li, and Y. Y. Gao, Phys. Rev. C **70**, 034610 (2004); B. A. Li, P. Danielewicz, and W. G. Lynch, *ibid.* **71**, 054603 (2005); X. F. Luo, X. Dong, M. Shao, K. J. Wu, C. Li, H. F. Chen, and H. S. Xu, *ibid.* **76**, 044902 (2007); B. A. Li, W. Chen, and C. M. Ko, Phys. Rep. **464**, 113 (2008).

[10] C. Hartnack, L. Zhuxia, L. Neise, G. Peilert, A. Rosenhauer, H. Sorge, J. Aichelin, H. Stocker, and W. Greiner, Nucl. Phys. **A495**, 303 (1989); C. Hartnack, Ph.D. thesis, University of Frankfurt, Frankfurt, Germany, GSI Report No. 93-5 (1993) (unpublished); C. Hartnack, J. Aichelin, H. Stöcker, and W. Greiner, Mod. Phys. Lett. A **9**, 1151 (1994); Phys. Lett. **B336**, 131 (1994); S. Soff, S. A. Bass, C. Hartnack, H. Stöcker, and W. Greiner, Phys. Rev. C **51**, 3320 (1995); C. Hartnack, R. K. Puri, J. Aichelin, J. Konopka, S. A. Bass, H. Stöcker, and W. Greiner, Eur. Phys. J. A **1**, 151 (1998).

[11] C. Hartnack, H. Oeschler, and J. Aichelin, Phys. Rev. Lett. **90**, 102302 (2003); J. Phys. G **35**, 044021 (2008).

[12] H. Kruse, B. V. Jacak, and H. Stöcker, Phys. Rev. Lett. **54**, 289 (1985); J. J. Molitoris and H. Stöcker, Phys. Rev. C **32**, 346(R) (1985); J. Aichelin and G. Bertsch, Phys. Rev. C **31**, 1730 (1985).

[13] C. Hartnack and J. Aichelin, J. Phys. G **28**, 1649 (2002); **30**, s531 (2004).

[14] S. A. Bass, C. Hartnack, H. Stöcker, and W. Greiner, Phys. Rev. C **51**, 3343 (1995); B. J. VerWest and R. A. Arndt, Phys. Rev. C **25**, 1979 (1982).

[15] D. J. Magestro, W. Bauer, and G. D. Westfall, Phys. Rev. C **62**, 041603(R) (2000); E. Lehmann, A. Faessler, J. Zipprich, R. K. Puri, and S. W. Huang, Z. Phys. A **355**, 55 (1996); A. D. Sood

and R. K. Puri, Phys. Rev. C **73**, 067602 (2006); **70**, 034611 (2004).

[16] C. Y. Wong, *Introduction to High-Energy Heavy Ion Collisions* (World Scientific, Singapore, 1994).

[17] S. Kumar, R. K. Puri, and J. Aichelin, Phys. Rev. C **58**, 1618 (1998); C. Liewen, Z. Fengshou, and J. Genming, Phys. Rev. C **58**, 2283 (1998); K. Chen, Z. Fraenkel, G. Friedlander, J. R. Grover, J. M. Miller, and Y. Shimamoto, Phys. Rev. **166**, 949 (1968).

[18] J. K. Dhawan and R. K. Puri, Eur. Phys. J. A **33**, 57 (2007).

[19] T. Z. Yan, X. G. Ma, X. Z. Cai, D. Q. Feng, W. Guo, C. W. Ma, W. Q. Shen, W. D. Tian, and K. Wang, Chin. Phys. **16**, 2676 (2007).

[20] R. E. Renfordt *et al.*, Phys. Rev. Lett. **53**, 763 (1984).

[21] W. Reisdorf *et al.*, Phys. Rev. Lett. **92**, 232301 (2004).

[22] W. Reisdorf *et al.*, Phys. Lett. **B595**, 118 (2004).